Polymer Bulletin

Mechanical Properties of Biodegradable Polyhydroxyalkanoates/Single Wall Carbon Nanotube Nanocomposite Films

Seok Il Yun (✉)**, Gerry E. Gadd, Bruno A. Latella, Victor Lo, Robert A. Russell, Peter J. Holden**

Australian Nuclear Science and Technology Organisation, PMB 1, Menai, NSW 2234, Australia
E-mail: siy@ansto.gov.au; Fax: 61 2 9717 9286

Summary

The nanocomposite films of poly(3-hydroxybutyrate) (PHB) and poly(3-hydroxy-octanoate) (PHO) with single wall carbon nanotubes (SWCNTs), were prepared. The Optical microscopy showed that the crystalline size substantially decreased for PHB/SWCNTs nanocomposites with a 1 % weight fraction of SWCNTs relative to PHB (PHB/(1%)SWCNTs), indicating the effective nucleation of PHB crystallization by SWCNTs. Mechanical properties of the nanocomposite films were measured by nanoindentation. Both polymer nanocomposite films showed an increase in hardness (H) and Young's modulus (E), with SWCNTs concentration. The PHB/SWCNTs nanocomposite films are found to be more brittle than neat PHB films.

Introduction

Nanocomposites of biopolymers with nano-fillers such as carbon nanotubes or clay, offer significant potential for their increased utilization, as a result of the improvements in mechanical and thermal properties [1-9]. Enhanced mechanical strength has been reported for organoclay nanocomposites of biodegradable polymers such as polylactide, cellulous acetate and poly(butylene succinate) [1-4]. With regards to biopolymers, polyhydroxyalkanoates (PHAs) have become one of the most interesting biomaterials for application in tissue engineering [10]. PHAs are natural, linear, thermoplastic polyesters synthesized by micro-organisms as intracellular carbon reserves and ion sinks in response to limited nutrient availability and imposed stress conditions. More than 100 different known types of PHA monomers have been reported depending on the number of carbon atoms and functional groups in the monomer [11]. The members of the PHA family encompass a wide range of mechanical properties, from hard and brittle poly(3-hydroxybutyrate) (PHB) to soft and elastomeric poly(3-hydroxyoctanoate) (PHO). However, PHB is the most studied polymer from the PHA family. The natural occurrence of low molecular weight PHB in human blood as well as its degradation product, 3-hydroxybutyric

acid, being a common metabolite in all higher living beings, is direct support for it being non toxic in regards to implantation [12,13]. The PHB/hydroxyapatite composite has been found to have increased mechanical strength as compared to the neat polymer PHB, and has also exhibited bioactivity in another related investigation [5,6]. PHB reinforced with Bio-glass has also shown an increased Young's modulus as well as hardness [7]. In this paper, we report on the mechanical properties of PHB and PHO nanocomposite films with SWCNTs. Carbon nanotube-based biopolymer composites have drawn interest due to the improved electric current conductivity as well as their mechanical properties. It has been reported that electrical stimulation through current-conducting nanotube/polylactic acids composites improved the various functions that are responsible for the chemical composition of the organic and inorganic phases of bone as well as increasing their rate of proliferation offering new avenues for stimulation of bone repair [8]. The possible utilization of biocompatible multi wall nanotube-based three dimensional matrixes as scaffolds for cellular growth has also been suggested and studied [9]. However, to our knowledge, no report has been made of mechanical properties of carbon nanotube based PHA composites. The CNT reinforced PHA composites may provide enhanced cellular proliferation, while improving the bioresorbability after the scaffold has performed its function. The current-conductivity of the composites may also benefit PHB fibers used as neutral scaffolds [10]. We prepared nanocomposite films of PHB and PHO, with the specific SWCNTs concentrations of 0, 1 and 10 wt% for each polymer. The mechanical properties of the nanocomposite films were subsequently measured using nano-indentation experiments.

Experimental Procedures

Preparation of Polymers

PHB was sourced commercially (Aldrich), but PHO was synthesized through fed-batch cultivation of *Pseudomonas oleovorans* using octanoic acid (Sigma, Australia) as the carbon source. Synthetic procedures were similar to the previous method to produce deuterated PHO [14]. An enrichment culture in LB broth [15] was pelleted and resuspended in a small volume (50mL) of Modified E medium [16]. The cells were acclimated for 3 hours prior to inoculation into a 2L fermentor (BBraun, Germany) containing 1.5L of Modified E medium, with 20mM octanoic acid. Biomass was grown at 30°C with forced aeration and impeller speed at 600rpm until the octanoate was depleted. Dissolved Oxygen was then maintained below 20% by reducing the impeller speed and adding aliquots of octanoic acid, creating suitable conditions for formation of PHO inclusions. PHO polymer was prepared from lyophilised cell biomass through chloroform extraction, and purified by precipitation in hexane and cold methanol. The polymer was cut into accurately weighed pieces and dissolved as described below.

Preparation of Polymer/Carbon nanotubes Composite Films

The PHO/SWCNTs and PHB/SWCNTs composites with the three SWCNTs composition, 0, 1 and 10 wt%, were prepared by a solvent-casting method using chloroform as a co-solvent. PHO 2% in chloroform was prepared at room tempera-

ture. Since the commercial PHB did not dissolve in chloroform at room temperature, PHB 2% in chloroform was prepared at 70°C. The single wall carbon nanotubes were purchased from SES Research (USA). They had a typical diameter of 1.2-1.4 nm and a range of length from 5 to 100 nm.

The carbon nanotubes solutions (2% in chloroform) were added to PHO and PHB solutions followed by high power sonication of SWCNTs/PHB, PHO solutions for 1 min. Since the slow solvent evaporation leads to agglomeration of SWCNTs, SWCNTs/PHB, PHO solutions were dropped onto a hot glass (60°C) in order to reduce evaporation time. The composite films were dried in the vacuum oven at 60°C for 12 hours and the thickness of the films was a few micrometers by stylus profilometry.

Gas Chromatography-Mass Spectrometry Measurement

Biomass containing PHO inclusions was lyophilised, and then refluxed in acidified methanol to form methyl esters for analysis by Gas Chromatography-Mass Spectrometry (GC-MS). The derivatised samples were analysed using a Varian GC 3900 coupled to a Varian 1200 MS (Varian, Melbourne, Australia). 1μL of sample was injected onto a VF-5ms capillary column (30m/ 0.32mm i.d./μm film) with a split ratio of 100:1. The column was held at 40°C for 3 minutes then ramped to 250°C (20°C/min) and held for 1.5 min. The ionising energy for electron impact MS was 70eV.

Nanoindentation Measurement

Indentation tests were also performed on PHO and PHB composite films on glass substrate. An instrumented ultramicro-indentation system (UMIS 2000, CSIRO Australia) configured with a Berkovich diamond indenter was used to produce the indentations. Calibration of the indenter tip shape was carried out using fused silica glass (elastic modulus, $E = 70$ GPa and $v = 0.2$) at peak loads, P_{max}, ranging from 0.2 to 500 mN, to provide an accurate tip profile as a function of penetration depths. The indentation loads and the corresponding displacements were recorded continuously throughout a loading-unloading cycle, enabling measurement of the elastic modulus and hardness of the indented specimen. The indentation load increases with 20 increments up to $P_{max} = 2$ mN for PHO films and 10mN for PHB films with a dwell at P_{max} of 10 seconds followed by unloading with 20 decrements. At least 20 indentations were made in a number of random locations on each film. The hardness and elastic modulus were determined from the slope, dP/dh, and penetration depth at maximum load, P_{max}, from the unloading curve. Knowledge of the indenter geometry and from the penetration depth, the contact area, A, could be determined from which the hardness, H, could be calculated: [17]

$$H = P_{max}/A \qquad \textbf{(1)}$$

The effective elastic modulus is given by: [18]

$$E^* = \frac{dP}{dh}\frac{1}{2}\frac{\sqrt{\pi}}{\sqrt{A}} \qquad \textbf{(2)}$$

The Young's modulus, E, of the specimen is then obtained from the relation: [17]

$$\frac{1}{E^*} = \frac{1-v^2}{E} + \frac{1-v_i^2}{E_i}$$

(3)

where v is Poisson's ratio of the specimen (assumed $v = 0.3$) with E_i (1141 GPa) and v_i (0.07) the elastic constants of the diamond indenter.

Results and Discussion

Commercial PHB consisted solely of the C4 monomer, whereas the medium chain length (mcl) PHA consisted primarily of PHO (84%) with minor amounts either with two carbons less or two carbons more than the alkanoic substrate (Fig. 1). This is due to enzymatic cleavage and removal of β-acetoacetate in the former case and acetyl-CoA addition in the latter, as observed in the poly β-hydroxybutyrate pathway [19].
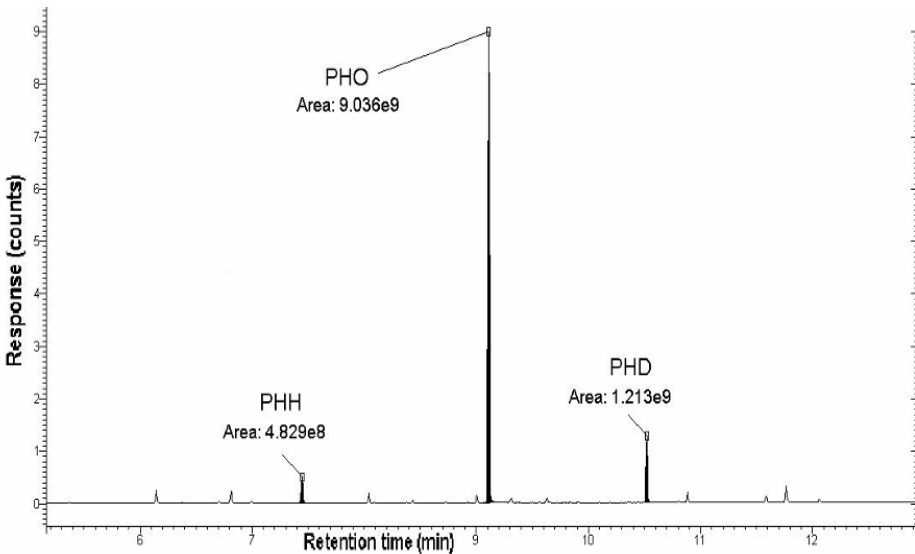

Fig. 1 GC-MS spectrum of mcl-PHAs produced by *Pseudomonas oleovorans* from octanoic acid

The crystalline behaviour of PHB composite films was qualitatively observed by optical microscopy measurements in cross polar mode as shown in Fig. 2. A large size of PHB crystalline phase with grain boundaries was observed from neat PHB (Fig. 2a), but SWCNTs significantly changed PHB crystalline behaviour (Fig. 2b, c). Crystallization behaviour of semicrystalline polymer/nanotubes composites is interesting because the nanotubes have the ability to nucleate the polymer crystallization. For polypropylene/(0.6~0.8%) SWCNTs, it was reported that the

SWCNTs successfully nucleate crystallization of polypropylene with the size and crystallization half time of spherulite substantially reduced [20]. It was also demonstrated that 0.1 % SWCNTs in poly(vinyl alcohol) also distinctively nucleated the PVA crystallization [21]. The large aggregates are seen for 1% SWCNTs in the optical microscopes without cross-polarization in Fig 3b indicating that SWCNTs did not well dispersed in PHB matrix. Regardless of the poor distribution of SWCNTS, Fig. 2b shows that 1% SWCNTs dramatically increase the number of nucleation sites and thereby decreased the average crystallite size of PHB. However the issue of transcrystalline phase was not studied in this paper. Even modest nanotube agglomeration decreases the aspect ratio leading to poor mechanical reinforcement. The uniform distribution of nanotubes is the most critical issue in fabricating CNT/polymer composites due to the strongly aggregating nature of CNT. Fabricating methods to improve dispersion of SWCNTs in PHB matrices are currently under investigation in our laboratory - particularly the use of spray-drying [22]. The crystalline size seems to increase for 10% SWCNTs compared to 1% SWCNTs as shown in Fig 2c. Comparing the optical micrographs for 1% and 10% composites (Fig 3b, c), the size of aggregates for 10% SWCNTs is substantially larger than 1% SWCNTs. The results show that 10% SWCNTs did not nucleate as effectively as 1% due to the large degree of aggregation of the nanotubes.
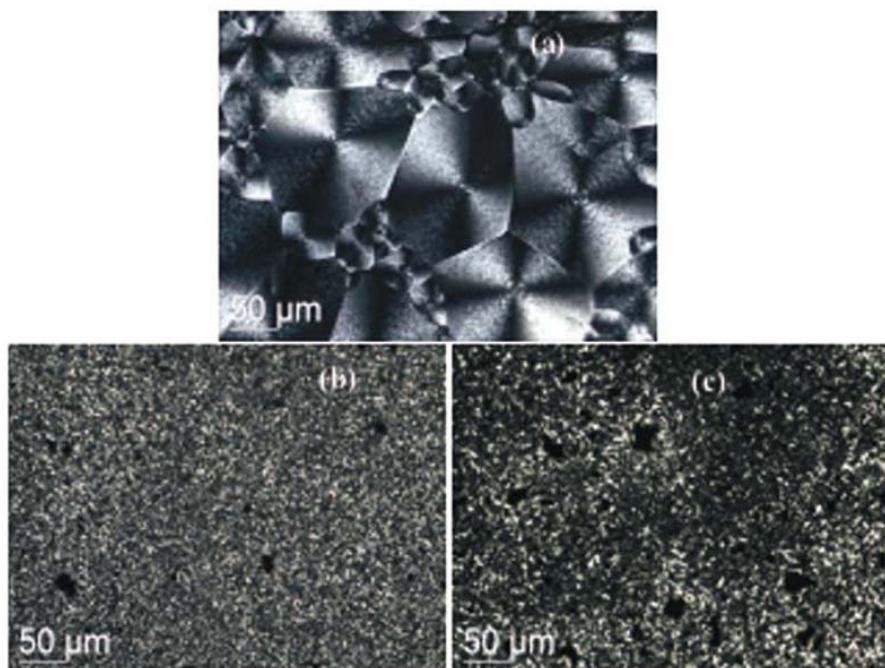

Fig. 2 Optical micrograph (transmission mode with cross-polar) of (a) neat PHB (b) PHB/1% SWCNTs (c) PHB/10% SWCNTs
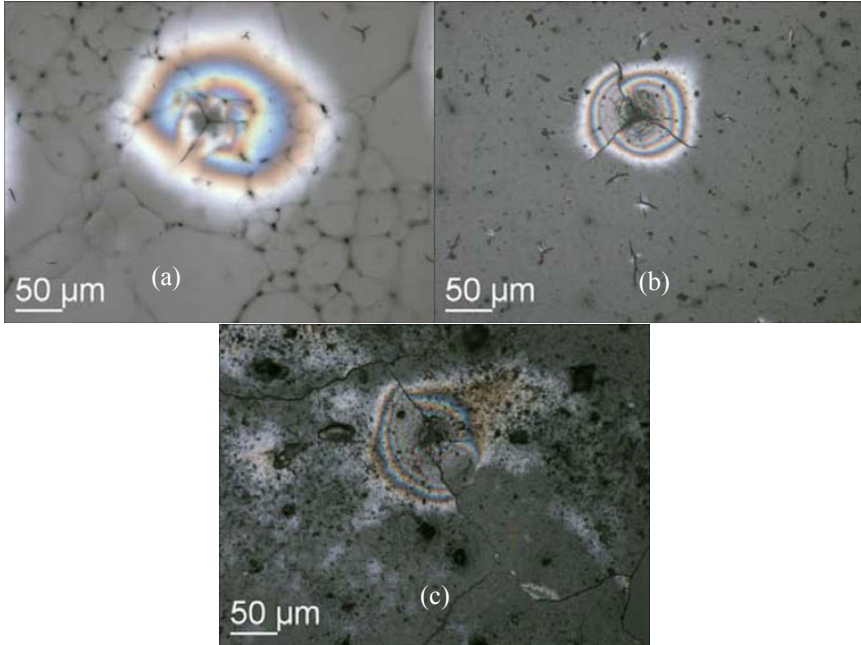
Fig. 3 Optical micrographs showing 400 mN indentations of: (a) neat PHB and (b) PHB/1% SWCNTs (c) PHB/10% SWCNTs
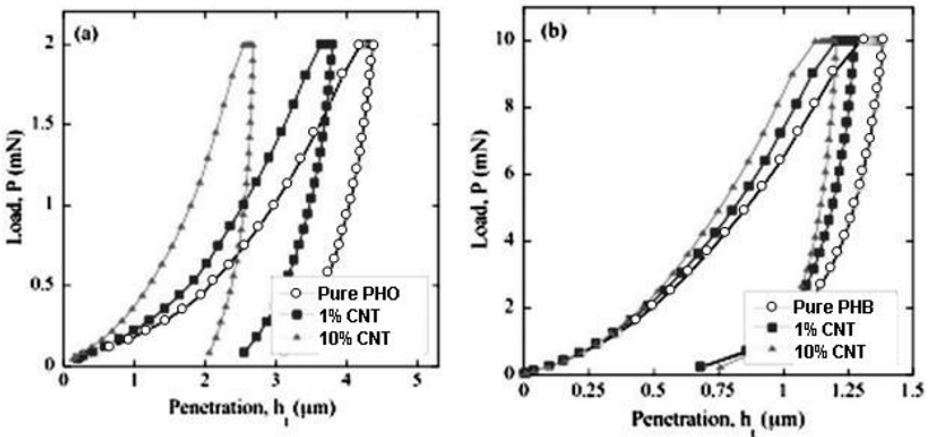

Fig. 4 Indentation load-displacement curves for the (a) PHO and (b) PHB films

The average load–displacement plots from the nanoindentation data for the PHO and PHB films are given in Fig. 4. In Fig. 4(a) it is clear that the addition of 1% and 10% SWCNTs to PHO shifts the loading curves towards the left, which is indicative of lower plastic deformation and hence increased hardness (see later). This trend was also apparent in the PHB films (Fig. 4(b)) but the differences in the load–displacement curves of the neat, 1% and 10% SWCNT were noticeably less.

Table 1. Young's Modulus (E) and hardness (H) measured by the nanoindentation method.

	PHB films			PHO films		
	SWCNTs content (%)			SWCNTs content (%)		
	0	1	10	0	1	10
H (GPa)	0.31 ± 0.01	0.33 ± 0.01	0.35 ± 0.01	$(5.6 \pm 0.06) \times 10^{-3}$	$(7.7 \pm 0.1) \times 10^{-3}$	$(13.7 \pm 0.6) \times 10^{-3}$
E (GPa)	5.66 ± 0.17	7.62 ± 0.17	11.74 ± 0.64	0.12 ± 0.01	0.15 ± 0.01	0.53 ± 0.05
H/E	0.055 ± 0.004	0.043 ± 0.003	0.030 ± 0.004	0.048 ± 0.004	0.052 ± 0.003	0.026 ± 0.004

Table 1 summarizes the Young's modulus (E) and hardness (H) of the films obtained from the nanoindentation measurements. The values in Table 1 are the averages obtained from up to 20 indentation test data on each sample. The hardness and Young's modulus of PHB and its composites are significantly larger than that of PHO based composites as illustrated in Fig. 4 by the larger penetration depths at lower loads for the PHO films. The Young's modulus increased as a function of SWCNTs concentration for both PHO and PHB composites. The increase in hardness was found to be minimal for PHB composites compared with PHO composites. To obtain an understanding of the fracture damage and the degree of cracking in the films several higher indentation loads, 400-500 mN were used to initiate cracking in the PHB films, although no quantitative measurement of fracture toughness was done due to possible substrate effects at these loads. The same loading–unloading procedure was used as per the low load indents with the Berkovich indenter. The impressions were then examined using an optical microscope as shown in Fig. 3. For the neat PHB radial cracks were suppressed (Fig. 3(a))   whereas small radial cracks were evident in the 1% composite (Fig. 3(b)). However well-developed, long radial cracks emanating from the impression corners were apparent for PHB/(10%)SWCNTs (Fig. 3(c)). The long radial cracks indicated lower toughness. These results, although qualitative clearly indicate that PHB becomes more brittle with increasing SWCNTs concentrations. The high brittleness of PHB polymers have been a major issue and attributed to the higher degree of crystallinity [23]. The PHB composites become more brittle although the crystalline size of PHB substantially decreased when blended with carbon nanotubes. Brittleness of the materials is usually defined by B = H/T where (B; brittle index, H; hardness, T; toughness) [24]. Brittleness of SWCNTs composites may be caused by the increased hardness of the composites as shown in Table 1. However a relatively small H increase may not be the only reason for such a huge cracking for PHB/(10%)SWCNTs. As seen in Fig. 3 (c) the aggregates were large for PHB/(10%)SWCNTs compared with PHB/(1%)SWCNTs. It is also possible that large agglomerates of nanotubes may act as stress concentrators and results in degraded toughness properties of the composite film. The hardness/elastic modulus ratio is useful in describing the deformation of materials [24-26]. As shown in Table 1, the H/E ratio for 1% SWCNTs composites was similar to neat PHO or PHB films, but much smaller for PHB/(10%)SWCNTs films, which suggests that the fundamental deformation mechanisms of PHB/(10%)SWCNTs films are different

from neat PHB and PHB/(1%)SWCNTs. The deformation behaviour may be strongly influenced by the SWCNT clusters and aggregation in the PHB/(10%)SWCNTs films, rather than the structure of the matrix and its interface with SWCNTs.

Conclusions

Nanocomposite films of poly(3-hydroxybutyrate) (PHB) and poly(3-hydroxy-octanoate) (PHO) with single wall carbon nanotubes (SWCNTs), were prepared by solution casting on the hot substrate (60°C). Optical microscopy showed that a 1 % of SWCNTs relative to PHB (PHB/(1%)SWCNTs), effectively nucleate PHB crystallization although carbon nanotubes did not well dispersed in PHB. The 10 % of SWCNTs (PHB/(10%)SWCNTs) was less effective in nucleating the crystallization due to a large agglomeration of SWCNTs compared to 1 % of SWCNTs. Although both polymer nanocomposite films showed an increase in hardness (H) and Young's modulus (E), with SWCNTs concentration, the increase was found to be more significant for PHO nanocomposites. The PHB/SWCNTs nanocomposite films are found to be more brittle than neat PHB films.

References

1. Nam, J. Y.; Ray, S. S.; Okamoto, M. Macromolecules 2003, 36, 7126.
2. Krikorian, V.; Pochan, D. J. Macromolecules 2005, 38, 6520.
3. Park, H.-M.; Liang, X.; Mohanty, A. K.; Misra, M.; Drzal, L. T. Macromolecules 2004, 37, 9076.
4. Ray, S. S.; Okamoto, K.; Okamoto, M. Macromolecules 2003, 36, 7126.
5. Knowles, J. C.; Hastings, G. W.; Ohta, H.; Niwa, S.; Boeree, N. Biomaterials 1992, 13, 491.
6. Luklinska, Z. B.; Bonfield, W. J. J. Mater. Sci.; Mater. Med. 1997, 8, 379.
7. Rezwan, K.; Chen, Q. Z.; Blaker, J. J.; Boccaccini, A. R. Biomaterials 2006, 27, 3413.
8. Supronowicz, P. R.; Ajayan, P. M.; Ullmann, K. R.; Arulanandam, B. P.; Metzger, D. W.; Bizios, R. J. Biomed. Mater. Res. 2002, 59, 499.
9. Correa-Duarte, M. A.; Wagner, N.; Rojas-Chapana, J.; Morsczeck, C.; Thie, M.; Giersig, M. Nano Lett. 2004, 4, 2233.
10. Chen, G.-Q.; Wu, Q. Biomaterials 2005, 26, 6565.
11. Steinbüchel, A. Macromol. Biosci. 2001, 1, 1.
12. Gogolewski, S.; Jovanovic, M.; Perren, S. M.; Dillon, J. G.; Hughes, M. K. J. Biomed. Mater. Res. 1993, 27, 1135.
13. Reusch, R. N.; Sparrow, A. J.; Gardiner, J. Biochim. Biophys. Biophys. Acta 1992, 1123, 33.
14. Foster, L. J. R.; Russell, R. A.; Sanguanchaipaiwong, V.; Stone, D. J. M.; Hook, J. M.; Holden, P. J. Biomacromolecules 2006, 7, 1344.
15. McCool, G. J.; Fernandez, T.; Li, N.; Cannon, M.C. FEMS Microbiol. Lett. 1996, 138, 41.
16. Vogel, H.; Bonner, D. J. Biol. Chem. 1956, 218, 97.
17. Oliver W. C.; Pharr G. M. J. Mater. Res. 2004, 19, 3.
18. Fischer-Cripps, A. C. Surf. Coat. Technol. 2006, 200, 4153.
19. Curley, J. M.; Lenz, R.W.; Fuller, R. C. Int. J. Biol. Macromol.1996, 19, 29.
20. Bhattacharyya, A. R.; Sreekumar, T. V.; Kumar, S.; Ericson, L. M.; Hauge, R. H.; Smalley, R. E. Polymer 2003, 44, 2373.
21. Probst, O.; Moore, E. M.; Resasco, D. E.; Grady, B. P. Polymer 2004, 45, 4437.

22. Yun, S. I.; Attard, D.; Lo, V.; Davis, J.; Li, H.; Latella, B.; Tsvetkov, F.; Noorman, H.; Moricca, S.; Knott, R.; Hanley, H.; Morcom, M.; Simon, G. P.; Gadd, G. E. J. Appl. Polym. Sci. 2008, 108, 1550
23. Azuma, Y.; Yoshie, N.; Sakurai, M.; Inoue, Y.; Chujo, R. Polymer 1992, 33, 4763.
24. Lawn B. R. In Fracture of brittle solids. London: Cambridge University Press, 1993; chap. 8.
25. Lawn, B. R.; Howes V. R. J. Mater. Sci. 1981, 16, 2745
26. Marshall, D. B.; Noma, T.; Evans, A. G. J. Am. Ceram. Soc. 1982, 65, C175